Thermal conductivity of a laser plasma

Nathaniel R. Shaffer [1,*] Andrei V. Maximov,[1,2] and Valeri N. Goncharov[1,2]

[1]*Laboratory for Laser Energetics, University of Rochester, Rochester, New York 14623, USA*
[2]*Department of Mechanical Engineering, University of Rochester, Rochester, New York 14623, USA*

We present a model of the electron thermal conductivity of a laser-produced plasma. The model, supported by Vlasov-Fokker-Planck simulations, predicts that laser absorption reduces conductivity by forcing electrons out of a Maxwell-Boltzmann equilibrium, which results in the depletion of both low-velocity bulk electrons and high-velocity tail electrons. We show that both the bulk and tail electrons approximately follow super-Gaussian distributions, but with distinct exponents that each depend on the laser intensity and wavelength through the parameter $\alpha = Z v_E^2 / v_T^2$. For a value of $\alpha = 0.5$, tail depletion reduces the thermal conductivity to half its zero-intensity value. We present our results as simple analytic fits that can be readily implemented in any radiation-hydrodynamics code or used to correct the local limit of nonlocal conduction models.

I. INTRODUCTION

Thermal conduction is a key component of the energy balance and transport of laser-produced plasmas, especially those produced in high-energy-density experiments such as high-performance inertial confinement fusion (ICF) implosions [1]. In laser direct drive (LDD) experiments, thermal conduction is responsible for converting laser energy absorbed in the corona into ablation pressure, providing the drive for a spherical implosion [2]. The more conductive the coronal plasma, the better the coupling between the laser and the target, which is beneficial for fusion performance. In laser indirect drive (LID), the laser illuminates the interior wall of a gas-filled hohlraum, which emits x rays that drive the capsule. The radiation transport properties throughout the hohlraum and blowoff plasma are sensitive to the temperature profile and thus to the thermal conductivity of the plasma [3,4].

The baseline model for thermal conduction in a plasma is that of Spitzer and Härm (SH) [5]. Not only is this the basic model used in radiation-hydrodynamics simulations, but it is also central to the construction of nonlocal conduction models [6–8]. The fundamental assumption underpinning this theory is that the electrons are in local thermodynamic equilibrium with a Maxwell-Boltzmann (MB) velocity distribution. However, the inverse bremsstralhung (IB) absorption of laser light distorts the electron distribution function away from a MB form, a phenomenon sometimes called the "Langdon effect" [9]. In this case, the SH theory no longer applies, and the local theory of heat conduction as well as nonlocal models based on SH need to be revised to explicitly account for laser absorption.

Some theoretical attempts have been made to assess how laser intensity affects heat conduction [10–12], but these have never precipitated a quantitative and practical model to re-

place the SH theory despite their dramatic predictions: that accounting for laser intensity leads to a reduction in the thermal conductivity by as much as a factor of four to five. The lack of this effect in mainline conduction models means would imply that current radiation-hydrodynamics simulations of laser-produced plasmas might seriously overestimate the conductivity in regions of high laser intensity, even before considering possible nonlocal effects. In the context of ICF experiments, this region corresponds to the coronal (LDD) or blowoff (LID) plasmas, where changes to the conductivity have compounding effects on the power balance and performance of ICF designs.

In this paper we resolve this issue by providing an accurate and practical model for the reduced thermal conductivity of a plasma in the presence of laser absorption. Our approach is based on a detailed model of the electron distribution function in the presence of absorption and conduction, supported by Vlasov-Fokker-Planck (VFP) simulations of the relaxation of long-wavelength temperature perturbations in a plasma absorbing laser light with fixed intensity. Electron-ion collisions, electron-electron collisions, and nonlinear absorption (Langdon effect) are all taken into account. The main result is that absorption reduces the thermal conductivity from the SH value according to

$$\frac{\kappa(Z, \alpha)}{\kappa_{SH}(Z)} = \frac{c_0(Z) + c_1(Z)\alpha}{1 + c_2(Z)\alpha}, \tag{1}$$

where

$$\kappa_{SH}(Z) = \frac{256\sqrt{2\pi}\epsilon_0^2 k_B^{\frac{7}{2}} T_e^{\frac{5}{2}}}{\sqrt{m_e} Z e^4 \Lambda_{ee}} \frac{Z + 0.24}{Z + 4.20} \tag{2}$$

is the SH conductivity [5],

$$\alpha = Z_{IB} \frac{v_E^2}{v_T^2} \tag{3}$$

*nsha@lle.rochester.edu

is the Langdon parameter, and

$$Z = \frac{\sum_i Z_i^2 n_i \Lambda_{ei}}{\sum_i Z_i n_i \Lambda_{ee}}, \quad Z_{IB} = \frac{\sum_i Z_i^2 n_i \Lambda_{IB,i}}{\sum_i Z_i n_i \Lambda_{ee}} \quad (4)$$

are the effective ion charge numbers for collisions and absorption, respectively. The quantities c_0, c_1, and c_2 are numerical coefficients which depend weakly on Z. In the above, Z_i, n_i, Λ_{ei}, and $\Lambda_{IB,i}$ are the charge state, number density, electron-ion Coulomb logarithm, and IB Coulomb logarithm [13,14] for ion species i, Λ_{ee} is the electron-electron Coulomb logarithm, $v_T = \sqrt{k_B T_e/m_e}$ is the electron thermal speed for temperature T_e, and $v_E = eE_L/(m_e \omega_L)$ is the electron oscillation velocity in a laser with angular frequency ω_L and electric field amplitude $E_L = \sqrt{2I/(c\epsilon_0)}$ for a laser with intensity I. Fundamental constants appearing in these expressions are the elementary charge e, the vacuum speed of light c, the vacuum permittivity ϵ_0, and the Boltzmann constant k_B. The parameter Z measures the relative strength of electron-ion to electron-electron collisions, which mainly affects the anisotropy of the distribution function responsible for the conduction. The parameter α measures the relative strength of IB absorption to electron-electron collisions, which mainly affects the shape of the isotropic part of the distribution function. The limit in which $Z \to \infty$ at fixed α corresponds to the Lorentz gas model, on which all prior theoretical work on this problem was based [10–12]. It will be seen that this treatment does capture the overall trend that conductivity reduces as α increases, but the reduction is significantly overestimated compared to a full kinetic treatment of electron-electron collisions.

II. SIMULATIONS

The VFP simulations were conducted using the code κ2, which expands the velocity dependence of the distribution function in spherical harmonics [15]. For the one-dimensional (1D) problems considered here, this is equivalent to a Legendre polynomial expansion, $f(x, \mathbf{v}, t) = \sum_{\ell=0}^{\infty} f_\ell(x, v, t) P_\ell(v_x/v)$, of which we retain only the isotropic component f_0 and flux component f_1. The two-term truncation is valid provided the temperature perturbation wavelength is much longer than the collision mean free path, otherwise the heat conduction is nonlocal. Convergence to the local limit is straightforward to establish by increasing the background electron density and verifying that the conductivity does not vary [16]. It is also necessary that the laser intensity not be so high that $v_E > v_T$, otherwise the laser absorption introduces temperature anisotropy [17,18].

The coupled VFP equations for the isotropic and anisotropic components of the distribution function are

$$\partial_t f_0 + \frac{v}{3}\partial_x f_1 - \frac{eE}{3m_e v^2}\partial_v(v^2 f_1) = C_0 + C_{IB}, \quad (5)$$

$$\partial_t f_1 + v\partial_x f_0 - \frac{eE}{m_e}\partial_v f_0 = -\nu_{ei}f_1 + C_1, \quad (6)$$

where C_0 and C_1 are respectively the isotropic and anisotropic electron-electron collision operators [19], C_{IB} is the IB absorption operator [9], $\nu_{ei}(v) = Ze^4 n_e \Lambda_{ee}/(4\pi\epsilon_0^2 m_e^2 v^3)$ is the velocity-dependent electron-ion collision rate, and E is the ambipolar electric field [20]. The Lorentz limit is obtained by excluding C_1 from the simulations. The results shown here were also checked using a more general VFP simulation
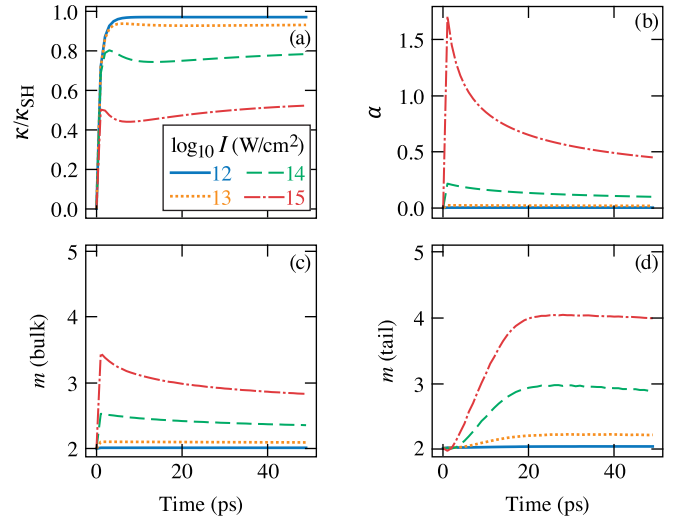
FIG. 1. Time evolution of a $Z = 10$ plasma at various laser intensities. (a) Conductivity reduction factor. (b) Langdon parameter. (c) Fitted super-Gaussian exponent for bulk electrons. (d) Fitted super-Gaussian exponent of tail electrons.

approach which treats the low- and high-frequency dynamics on equal footing, rather than relying on C_{IB} to model the absorption [20]. This gives a more accurate account of the IB absorption in principle, but we find for the simple laser fields considered here (uniform and constant) that the results are nearly identical to the conventional approach using C_{IB}.

The simulations are initialized with a MB distribution at fixed, uniform electron density and a sinusoidally perturbed temperature, $T_e(x, t = 0) = T_0 [1 + 10^{-3} \cos(2\pi x/L)]$, where $L = 5$ mm is the domain size and $T_0 = 200$ eV is the initial electron temperature. The electron density ranged from 0.1 to 1 times the critical density for 0.35-μm light as needed to ensure the long-wavelength limit was realized. The choice of a sinusoidal perturbation allows for periodic boundary conditions and facilitates using Fourier analysis to separate the evolution of the mean temperature from the fluctuating one. The laser intensity ramps up from zero to a uniform constant value over the first 100 fs of the simulation. As the simulation progresses, the mean temperature increases monotonically due to IB absorption, while the temperature fluctuation relaxes due to heat conduction. The instantaneous thermal conductivity is extracted from a Fourier analysis of the $k = 2\pi/L$ fundamental mode $\kappa = \text{Re}\{iQ_k/(kT_k)\}$, where Q_k is the Fourier component of the heat flux, $Q = 2\pi m_e/3 \int_0^\infty v^5 f_1 dv$, and T_k is the Fourier component of the temperature fluctuation.

The thermal conductivity obtained in this way varies in time because the mean temperature increases monotonically due to absorption. Consequently, the value of α also varies in time, as does the shape of f_0. The time evolution for a typical case is shown in Fig. 1, which shows the instantaneous values of κ/κ_{SH}, α, as well as super-Gaussian exponents characterizing the shape of f_0 (discussed further below). The thermal conductivity is only formally meaningful if the simulations have reached the hydrodynamic stage of evolution, meaning the time variation and space variation of the distribution function is totally implicit in the time variation and space variation of the temperature [21]. It is difficult to rigorously
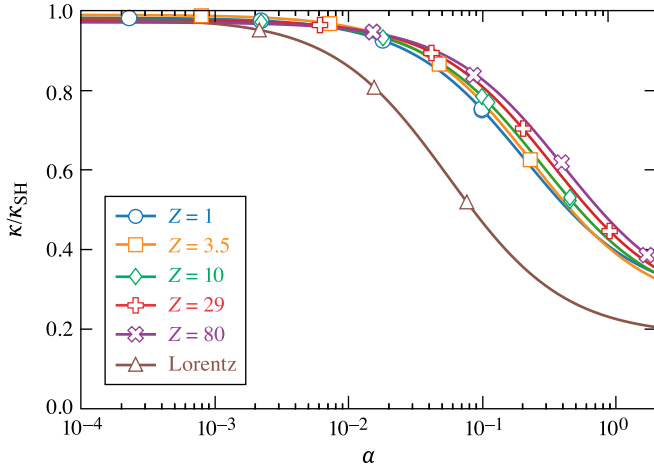
FIG. 2. Ratio of the thermal conductivity to the SH value as a function of Langdon parameter α for various ion charge numbers Z, as well as for a Lorentz gas. Symbols are the results of VFP simulations and lines are interpolation formulas.

identify whether or not this is the case in the VFP simulations. Nevertheless, Fig. 1 suggests two clear regimes: a transient relaxation up to about 10 ps and a quasisteady evolution from about 20 ps onward. Conservatively, we take only the last values of α and κ/κ_{SH} from each simulation to construct our model.

III. RESULTS AND DISCUSSION

The results are collected in Fig. 2, which shows the reduction in thermal conductivity as a function of α for various values of Z. Each data point is the final instantaneous values of κ/κ_{SH} and α obtained from a different value of the laser intensity ($I = 0, 10^{12}, 10^{13}, 10^{14}, 10^{15}$ W/cm^2). For each Z, the results are fitted to Eq. (1) and shown as solid lines; the resulting fit coefficients are given in Table I. Note that c_0 should in principle be unity, but we find it is systematically a few percent less, indicating that the zero-intensity thermal conductivity from VFP is slightly less than the SH value.

At nonzero intensity, the thermal conductivity is substantially reduced from the SH value. Even at small values of the Langdon parameter, $\alpha = 0.1$, the reduction is already about 25%, while at $\alpha = 1$, the reduction is almost 60%. This reduction exhibits only a weak dependence on Z, indicating that the reshaping of f_0 due to IB and the reshaping of f_1 due to electron-electron collisions are essentially separable effects. It is mainly the deformation of f_0 that causes the conductivity reduction, while the effect of electron-electron collisions on f_1 is not strongly intensity dependent. This insensitivity to Z might lead one to think that the Lorentz gas model should be adequate to describe the thermal conductivity reduction;

TABLE I. Fit coefficients for the conductivity reduction factor in Eq. (1).

	$Z = 1$	$Z = 3.5$	$Z = 10$	$Z = 29$	$Z = 80$	Lorentz
c_0	0.982	0.989	0.977	0.976	0.971	0.981
c_1	1.332	1.038	0.943	0.739	0.615	3.278
c_2	4.862	4.214	3.685	2.984	2.483	17.94
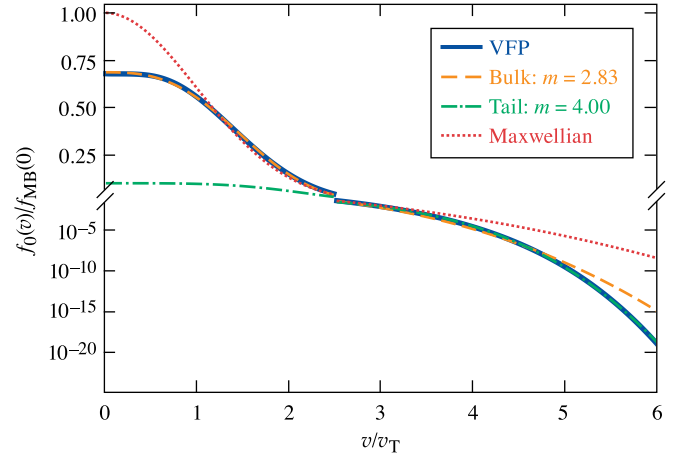
FIG. 3. Isotropic component of the velocity distribution function for a $Z = 10$ plasma with $\alpha = 0.45$. The solid line is the VFP result, the dashed line is a super-Gaussian fit to the bulk electrons, the dashed-dotted line is a super-Gaussian fit to the tail electrons, and the dotted line is a Maxwellian distribution. Note the transition from linear to logarithmic scale at $v = v_*$.

however, this turns out not to be the case. VFP results for the Lorentz gas severely overestimate the reduction in thermal conductivity. In the absence of a laser, the Lorentz gas model corresponds to the $Z \to \infty$ limit of the Spitzer-Härm conductivity, but this relationship no longer holds at nonzero intensity. In fact, when electron-electron collisions are fully accounted for, the trend is that at fixed α, higher-Z plasmas have a conductivity that is slightly closer to the SH value.

To better understand the failure of the Lorentz gas model, it is instructive to connect with the theory of Mora and Yahi [10]. The Mora-Yahi theory takes f_1 in steady state and neglects C_1 to obtain

$$f_1 = -\lambda_{ei}\left[\partial_x f_0 - \frac{eE}{mv}\partial_v f_0\right], \qquad (7)$$

where $\lambda_{ei} = v/\nu_{ei}$ is the mean free path. They consider f_0 to have a super-Gaussian form, $f_0(v) \propto \exp[-(v/v_m)^m]$, where the exponent m is assumed to be known. The thermal conductivity may then be determined analytically as a function of m, with $m = 2$ recovering the Lorentz gas limit of SH theory.

To connect with the VFP results, we must determine the value of m that best characterizes the shape of f_0 *in the velocity range relevant to conduction*. We emphasize the importance of choosing the appropriate velocity range because this has been a point of confusion in the past [11]. In the literature on IB absorption, there is both simulation and experimental support for relating the exponent to α as $m_{IB}(\alpha) = 2 + 3/(1 + 1.66/\alpha^{0.724})$, as proposed by Matte *et al.* [13,22–24]. However, IB absorption is sensitive only to the bulk electrons with $v \lesssim 3v_T$, and accordingly we find that this formula only describes the low-velocity population in our VFP simulations.

An illustrative example is shown in Fig. 3, which shows f_0 from VFP simulations, as well as super-Gaussian fits to the bulk and tail electron populations. Here, "bulk" refers to electrons with $v < v_*$ and "tail" to electrons with $v > v_*$, where v_* is the velocity where $f_1(v_*) = 0$. That is, the tail electrons are those flowing down the temperature gradient and con-
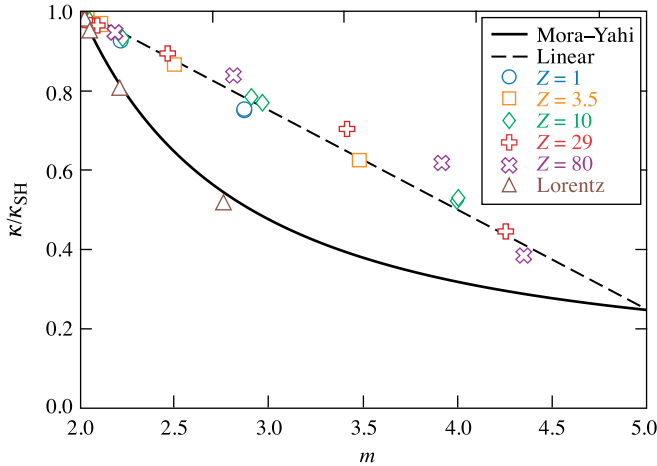
FIG. 4. Ratio of the thermal conductivity to the SH value as a function of the super-Gaussian exponent of the tail electrons. Symbols are VFP results for various charge numbers Z, as well as for a Lorentz gas. The solid curve is the Mora-Yahi theory.

tributing positively to the thermal conductivity, while the bulk electrons are those which form the neutralizing return current and contribute negatively to the thermal conductivity. The bulk and tail are characterized by different super-Gaussian exponents. The bulk agrees well with the Matte *et al.* model, which gives $m_{IB}(0.45) = 2.76$ in the case shown in Fig. 3. This implies that the collisional bulk electrons are insensitive to the presence of heat flow, and their energy distribution is described well with standard IB theory. The tail, however, is more sharply non-Maxwellian, with $m = 4$ being the best-fit value. This implies that the tail electron population is more depleted (and the thermal conductivity reduction more severe) than one would predict using m_{IB}. Evidently, a separate model for the tail electron distribution is needed.

Using the tail exponent fitted from each VFP simulation, the Mora-Yahi theory is evaluated and compared to the VFP simulation result in Fig. 4, which shows the thermal conductivity reduction as a function of the tail exponent. Strikingly, all the VFP simulations which properly account for electron-electron collisions on f_1 collapse in a way that suggests that κ/κ_{SH} is a universal function of m. Though m generally depends on both Z and α, the Z dependence is weak, and we find that a Z-independent expression of the same form used for IB,

$$m(\alpha) = 2 + 3/(1 + 0.247/\alpha^{0.972}), \qquad (8)$$

approximates the tail exponent of the VFP simulations at any Z within 3% when $\alpha < 1$. The Lorentz-limit VFP results follow a different trend entirely but are in excellent agreement with the Mora-Yahi prediction. An interesting finding is that though the VFP results do not reach $m = 5$, they do appear to trend toward the $m = 5$ Mora-Yahi prediction. A simple linear fit connecting the $m = 2$ and $m = 5$ limits,

$$\frac{\kappa(m)}{\kappa_{SH}} = 1 - 0.251(m - 2), \qquad (9)$$

gives remarkably good agreement with the VFP results, the errors for all but one case being within 8% [25]. Note, however,

there is some compounding of errors when Eqs. (8) and (9) are used together, so that applications requiring accuracy better than a few percent might prefer to interpolate the coefficients in Table I for use in Eq. (1).

In the theory of IB, $m = 5$ is an upper limit obtained when C_0 is neglected [9]. The trend of VFP toward Mora and Yahi's $m = 5$ prediction indicates that the Lorentz limit is only realized when *all* electron-electron collisions are neglected, not just those acting on f_1. One important implication for VFP [15,26–28] and simplified kinetic models [6,29–31] of laser plasmas is that one cannot neglect C_1 unless one is also willing to neglect C_0. This goes against a widespread practice to neglect C_1 and compensate by rescaling ν_{ei} to recover the SH conductivity in the local transport limit. This is done because C_1 is cumbersome to invert, making it both a computational bottleneck for VFP codes and inconvenient for analytic theory. This procedure, while tempting, totally misrepresents the effect of IB absorption on the heat flow and produces the wrong local transport limit at nonzero intensity.

IV. CONCLUSIONS

In summary, we have determined the thermal conductivity and equilibrium distribution function of a plasma heated by a laser using VFP simulations. In doing so, we have shown the importance of retaining an accurate and fully kinetic model of absorption and electron-electron collisions. This allowed us to identify important shortcomings of previous attempts to determine the thermal conductivity of a laser plasma. Specifically, in this work, the Lorentz approximation was eschewed and no functional form for the isotropic distribution function was assumed. The results can be represented analytically in a simple form which can be straightforwardly implemented in radiation-hydrodynamics codes and nonlocal conduction models as an intensity-dependent correction to the SH conductivity. The impact of this reduced conductivity on coupling efficiency in ICF experimental design will require thorough study and be the subject of future work.

[1] S. Atzeni and J. Meyer-ter-Vehn, *The Physics of Inertial Fusion* (Oxford Science, Oxford, UK, 2009).

[2] R. S. Craxton, K. S. Anderson, T. R. Boehly, V. N. Goncharov, D. R. Harding, J. P. Knauer, R. L. McCrory, P. W. McKenty, D. D. Meyerhofer, J. F. Myatt, A. J. Schmitt, J. D. Sethian, R. W. Short, S. Skupsky, W. Theobald, W. L. Kruer, K. Tanaka, R. Betti, T. J. B. Collins, J. A. Delettrez *et al.*, Phys. Plasmas **22**, 110501 (2015).

[3] N. B. Meezan, D. T. Woods, N. Izumi, H. Chen, H. A. Scott, M. B. Schneider, D. A. Liedahl, O. S. Jones, G. B. Zimmerman, J. D. Moody, O. L. Landen, and W. W. Hsing, Phys. Plasma **27**, 102704 (2020).

[4] W. A. Farmer, M. D. Rosen, G. F. Swadling, C. Bruulsema, C. D. Harris, W. Rozmus, M. B. Schneider, M. W. Sherlock, D. H. Edgell, J. Katz, and J. S. Ross, Phys. Plasmas **28**, 032707 (2021).

[5] L. Spitzer and R. Härm, Phys. Rev. **89**, 977 (1953).

[6] G. P. Schurtz, P. D. Nicolaï, and M. Busquet, Phys. Plasmas **7**, 4238 (2000).

[7] J. F. Luciani, P. Mora, and J. Virmont, Phys. Rev. Lett. **51**, 1664 (1983).

[8] J. R. Albritton, E. A. Williams, I. B. Bernstein, and K. P. Swartz, Phys. Rev. Lett. **57**, 1887 (1986).

[9] A. B. Langdon, Phys. Rev. Lett. **44**, 575 (1980).

[10] P. Mora and H. Yahi, Phys. Rev. A **26**, 2259 (1982).

[11] E. M. Epperlein and R. W. Short, Phys. Rev. E **50**, 1697 (1994).

[12] C. P. Ridgers, A. G. R. Thomas, R. J. Kingham, and A. P. L. Robinson, Phys. Plasmas **15**, 092311 (2008).

[13] D. Turnbull, J. Katz, M. Sherlock, L. Divol, N. R. Shaffer, D. J. Strozzi, A. Colaïtis, D. H. Edgell, R. K. Follett, K. R. McMillen, P. Michel, A. L. Milder, and D. H. Froula, Phys. Rev. Lett. **130**, 145103 (2023).

[14] R. Devriendt and O. Poujade, Phys. Plasmas **29**, 073301 (2022).

[15] M. Sherlock, J. P. Brodrick, and C. P. Ridgers, Phys. Plasmas **24**, 082706 (2017).

[16] In this paper, constant Coulomb logarithms are used throughout, so that the thermal conductivity is truly independent of density in the local limit.

[17] R. D. Jones and K. Lee, Phys. Fluids **25**, 2307 (1982).

[18] P. Porshnev, S. Bivona, and G. Ferrante, Phys. Rev. E **50**, 3943 (1994).

[19] M. Tzoufras, A. R. Bell, P. A. Norreys, and F. S. Tsung, J. Comput. Phys. **230**, 6475 (2011).

[20] N. R. Shaffer, M. Sherlock, A. V. Maximov, and V. N. Goncharov, Phys. Plasmas **30**, 043906 (2023).

[21] J. H. Ferziger and H. G. Kaper, *Mathematical Theory of Transport Processes in Gases* (North-Holland, Amsterdam, 1972).

[22] J. P. Matte, M. Lamoureux, C. Moller, R. Y. Yin, J. Delettrez, J. Virmont, and T. W. Johnston, Plasma Phys. Controlled Fusion **30**, 1665 (1988).

[23] D. Turnbull, A. Colaïtis, A. M. Hansen, A. L. Milder, J. P. Palastro, J. Katz, C. Dorrer, B. E. Kruschwitz, D. J. Strozzi, and D. H. Froula, Nat. Phys. **16**, 181 (2020).

[24] A. L. Milder, J. Katz, R. Boni, J. P. Palastro, M. Sherlock, W. Rozmus, and D. H. Froula, Phys. Rev. Lett. **127**, 015001 (2021).

[25] The case in question is for $Z = 80$ and $m = 4.34$, for which the error in Eq. (9) is 16%.

[26] E. M. Epperlein, J. Comput. Phys. **112**, 291 (1994).

[27] A. Sunahara, J. A. Delettrez, C. Stoeckl, R. W. Short, and S. Skupsky, Phys. Rev. Lett. **91**, 095003 (2003).

[28] R. J. Kingham and A. R. Bell, J. Comput. Phys. **194**, 1 (2004).

[29] V. N. Goncharov, O. V. Gotchev, E. Vianello, T. R. Boehly, J. P. Knauer, P. W. McKenty, P. B. Radha, S. P. Regan, T. C. Sangster, S. Skupsky, V. A. Smalyuk, R. Betti, R. L. McCrory, D. D. Meyerhofer, and C. Cherfils-Clérouin, Phys. Plasmas **13**, 012702 (2006).

[30] W. Manheimer, D. Colombant, and A. Schmitt, Phys. Plasmas **25**, 082712 (2018).

[31] A. Chrisment, P. Loiseau, J.-L. Feugeas, P.-E. Masson-Laborde, J. Mathiaud, V. Tikhonchuk, and P. Nicholaï, Phys. Plasmas **29**, 062301 (2022).